Pflugers Arch - Eur J Physiol (2012) 464:261–272
DOI 10.1007/s00424-012-1136-5

ION CHANNELS, RECEPTORS AND TRANSPORTERS

Involvement of TRPV1 and TRPV4 channels in migration of rat pulmonary arterial smooth muscle cells

Elodie Martin · Diana Dahan · Guillaume Cardouat · Jennifer Gillibert-Duplantier · Roger Marthan · Jean-Pierre Savineau · Thomas Ducret

Received: 13 June 2012 / Accepted: 26 June 2012 / Published online: 22 July 2012

Abstract Pulmonary hypertension, the main disease of the pulmonary circulation, is characterized by an increase in pulmonary vascular resistance, involving proliferation and migration of pulmonary arterial smooth muscle cells (PASMC). However, cellular and molecular mechanisms underlying these phenomena remain to be identified. In the present study, we thus investigated in rat intrapulmonary arteries (1) the expression and the functional activity of TRPV1 and TRPV4, (2) the PASMC migration triggered by these TRPV channels, and (3) the associated reorganization of the cytoskeleton. Reverse transcriptase–polymerase chain reaction (RT-PCR) analysis demonstrated expression of TRPV1 and TRPV4 mRNA in rat intrapulmonary arteries. These results were confirmed at the protein level by western blot. Using microspectrofluorimetry (indo-1), we show that capsaicin and 4α-phorbol-12,13-didecanoate (4α-PDD), selective agonists of TRPV1 and TRPV4, respectively, increased the intracellular calcium concentration of PASMC. Furthermore, stimulation of TRPV1 and TRPV4 induced PASMC migratory responses, as assessed by two different methods (a modified Boyden chamber assay and a wound-healing migration assay). This response cannot seem to be attributed to a proliferative effect as assessed by BrdU and Wst-1 colorimetric methods. Capsaicin- and 4α-PDD-induced calcium and migratory responses were inhibited by the selective TRPV1 and TRPV4 blockers, capsazepine and HC067047, respectively. Finally, as assessed by immunostaining, these TRPV-induced migratory responses were associated with reorganization of the F-actin cytoskeleton and the tubulin and intermediate filament networks. In conclusion, these data point out, for the first time, the implication of TRPV1 and TRPV4 in rat PASMC migration, suggesting the implication of these TRPV channels in the physiopathology of pulmonary hypertension.

Keywords Calcium · Cell viability · Migration · Proliferation · TRP channels · Vascular smooth muscle

Introduction

Pulmonary hypertension (PH) is a disease characterized by a progressive elevation of pulmonary arterial pressure leading to right heart failure and ultimately to death. From a pathobiological point of view, PH is a multifactorial disease characterized by a progressive increase in pulmonary vascular resistance caused, among others, by vasoconstriction, remodeling of the pulmonary vessel wall, and thrombosis [15]. In particular, sustained pulmonary vasoconstriction and remodeling of small pulmonary arteries (PA) are two key events of this disease [17, 28], both of which implicate pulmonary arterial smooth muscle cells (PASMC). Indeed, proliferation and migration of PASMC are involved in hyperreactivity of PA to contractile agonists, thickening of large pulmonary vessel medial wall, as well as in

Elodie Martin and Diana Dahan contributed equally to this work.

E. Martin · D. Dahan · G. Cardouat · J. Gillibert-Duplantier · R. Marthan · J.-P. Savineau · T. Ducret
Centre de Recherche Cardio-Thoracique de Bordeaux,
Univ Bordeaux,
33076 Bordeaux, France

E. Martin · D. Dahan · G. Cardouat · J. Gillibert-Duplantier · R. Marthan · J.-P. Savineau · T. Ducret
INSERM, U1045,
33076 Bordeaux, France

T. Ducret (✉)
Centre de Recherche Cardio-Thoracique de Bordeaux,
INSERM U1045, Université Bordeaux Segalen,
146 rue Léo-Saignat,
33076 Bordeaux Cédex, France
e-mail: thomas.ducret@u-bordeaux2.fr

muscularization of small pulmonary vessels [27]. As recently shown [4], the extension of PASMC into nonmuscularized vessels involves factors, such as serotonin, that stimulate PASMC proliferation and/or migration.

Cell migration plays a pivotal role in many physiological (including angiogenesis, embryonic morphogenesis, immune surveillance, tissue repair and regeneration…) and pathophysiological events (cancer, inflammation, mental retardation, osteoporosis, vascular disease…) (for review, see [29]). At the cellular level, cell migration is a multifactorial and multistep process that requires simultaneous changes in both cell morphology and adhesion [29] that depend on the intracellular calcium concentration ($[Ca^{2+}]_i$) [14, 21]. Indeed, a key step in the initiation of the process is an increase in $[Ca^{2+}]_i$, which results from a release of intracellular stored calcium and/or an influx of extracellular calcium. Intracellular released calcium is essentially originating from the sarcoplasmic reticulum, whereas calcium influx occurs through membrane channels with distinctive Ca^{2+} selectivity. Extracellular calcium ions can enter into smooth muscle cells following the activation of voltage-operated calcium channels (L- and T-type calcium channels), or nonselective cation channels (NSCC) that are permeable to calcium [11]. Part of NSCC belongs to the large family of transient receptor potential (TRP) proteins. TRP channels, that are activated by various chemical and physical stimuli, are characterized by six transmembrane-spanning domains, which form tetramers [25]. Based on structural homology, the TRP superfamily can be subdivided into seven main subfamilies: TRPC (“Canonical”), TRPV (“Vanilloid”), TRPM (“Melastatin”), TRPP (“Polycystin”), TRPML (“Mucolipin”), TRPA (“Ankyrin”), and TRPN (“NOMPC”). In PASMC, TRPC, TRPV, and TRPM are expressed [31, 35], and among the TRPV subfamily, TRPV1, TRPV2, and TRPV4 are the most abundantly expressed [35]. Interestingly, these three isoforms have been demonstrated to be the molecular basis of stretch-activated channels [16, 20, 22, 24, 30], and it was recently demonstrated that the activity of stretch-activated channels in PASMC was increased under chronic hypoxia [6, 37]. Moreover, we previously showed that serotonin, which stimulates bovine PASMC migration [4], activates a TRPV4-like current [5]. Finally, the involvement of TRPV1 in human hepatoblastoma (HepG2) cell migration [33] and in chronic hypoxia-induced proliferation of human PASMC [32] was already described. Thus, TRPV1 and TRPV4 may be required for PASMC migration occurring during PH.

In the present work, we focused our attention on TRPV1 and TRPV4 channels. We sought to identify TRPV1 and TRPV4 mRNA and proteins in rat intrapulmonary arteries using RT-PCR and western blot. Furthermore, we verified their functional activity by recording $[Ca^{2+}]_i$ responses (microspectrofluorimetric assay) elicited by capsaicin and 4α-phorbol-12,13-didecanoate (4α-PDD), selective agonists of TRPV1 and TRPV4, respectively, in PASMC. Finally, we also explored the role of these isoforms in PASMC migration (modified Boyden chamber and wound-healing assays), proliferation (BrdU incorporation), cell viability (Wst-1 assay), and cytoskeleton reorganization (immunostaining).

Materials and methods

Isolation of intrapulmonary arteries

Intrapulmonary arteries (IPA) were dissected from the lungs of male Wistar rats (250–350 g body weight), according to the animal care and use of our local ethics committee (Comité d'éthique régional d'Aquitaine). Briefly, the entire heart–lung preparation was rapidly removed en bloc. IPA of the first and second orders from the left lung were dissected free from surrounding connective tissues and endothelium (de-endothelialized IPA) under binocular control and sterile conditions.

RNA and cDNA synthesis

De-endothelialized IPA RNA from one rat was extracted using NucleoSpin® RNA XS kit according to the manufacturer’s instructions (Macherey-Nagel). Briefly, IPA were lysed by incubation in “lysis buffer” solution, in order to inactivate RNases and create appropriate binding conditions which favor adsorption of RNA to the silica membrane. After lysis, homogenization and reduction of viscosity were achieved by filtration with NucleoSpin® filter units. Residual genomic DNA was removed efficiently by time-saving on-column digestion with rDNase provided. Total RNA was eluted in RNAse-free water. The concentration of RNA was measured spectrophotometrically by GeneQuant RNA/DNA calculator (Amersham Pharmacia). The total RNA (1 μg) was reverse-transcribed into cDNA by using AMV reverse transcriptase (Promega) in the presence of RNase inhibitor and oligo d(T) as a primer at 42 °C for 60 min followed by heating at 94 °C for 3 min.

Polymerase chain reaction (PCR)

PCR was performed with a Rotor-Gene 2000 (Corbett Research) as previously described [2]. cDNA from 10 ng of total RNA was added to 0.2 μl of 50× Titanium Taq DNA Polymerase combined to its buffer (Clontech Laboratories), 1 mM dNTP, each of the appropriate primer (Sigma Genosys; see Table 1 for concentrations and sequences), and 0.5× SYBR Green (Molecular Probes). The reaction was initiated at 50 °C for 2 min, 95 °C for 10 min, and followed by 40 cycles of denaturation at 95 °C for 15 s and annealing/extension at 70 °C for 30 s. PCR negative

Table 1 Sequences of the primer pairs (S: sense; AS: antisense) are shown as well as GenBank accession number, product length, product Tm, and concentration for TRPV1 and TRPV4 genes

Gene	Sequence	GenBank accession number	Product length (bp)	Product Tm (°C)	Concentration (nM)
TRPV1	S: AGCGAGTTCAAAGACCCAGA AS: TTCTCCACCAAGAGGGTCAC	NM_031982.1	268	88.2	100
TRPV4	S: GCCACCCTACCCTTACCGTA AS: GGAAGGAGCCATCGACGAAGA	NM_023970.1	158	88.8	100

controls were systematically made by using water instead of cDNA. All specific primers were designed by using the primer analysis software (Oligo 6.6, Molecular Biology Insights). The efficiency of the PCR reactions was always more than 90 %. Specificity of the amplified PCR products was checked with melting curve analysis and by electrophoresis analysis on a 2 % agarose gel containing SYBR Green.

Western blot

De-endothelialized IPA were crushed and homogenized using RIPA buffer [1 % (*v*/*v*) Triton X-100, 1 % (*w*/*v*) Na deoxycholate, 150 mM NaCl, and 20 mM sodium or potassium phosphate, pH 7.2] with 5 mM EDTA and anti-protease cocktail (P8340; Sigma) for 1 h on ice. After scrapping, any insoluble material was removed by centrifugation at 15,000× *g* for 10 min at 4 °C, and the amount of proteins was assessed by the Lowry method. After heat denaturation during 6 min at 90 °C, equal amounts of proteins were subjected to electrophoresis on a 8–14 % acrylamide reducing gel. The proteins were transferred onto polyvinylidene fluoride membranes (Immobilon-P, Millipore) using a semi-dry electro-blotter (Bio-Rad) during 50 min. Unspecific sites were saturated using nonfat milk during 1 h and membranes were incubated overnight at 4 °C with diluted primary antibodies: rabbit anti-TRPV1 (1/400, Abcam) or rabbit anti-TRPV4 (1/400, Abcam). The membranes were then washed with a PBS–TWEEN 1 % buffer and treated with the corresponding horseradish peroxidase-linked secondary antibodies (anti-mouse or anti-rabbit, Pierce) for 2 h at room temperature. After several washes in PBS–TWEEN 1 % buffer, the membranes were processed for chemiluminescent detection using the Super Signal West Pico or Femto chemiluminescent substrate (Pierce), according to the manufacturer's instructions. Immunoblots were then revealed by enhanced chemiluminescence acquired using Kodak Image Station 4000 MM. Immunoblots were then stripped and revealed with mouse anti-β-actin (1/1,000, Sigma).

PASMC isolation and culture

As previously described [6], after isolation, de-endothelialized IPA were cut in several pieces (1×1 mm) and seeded on round glass coverslips for microspectrofluorimetry experiments or in Petri dishes for in vitro experiments. Explants were cultured in culture medium (Dulbecco's modified Eagle's medium (DMEM)–*N*-2-hydroxyethylpiperazine-*N*′-2-ethanesulfonic acid (HEPES) supplemented with 1 % penicillin–streptomycin, 1 % Na-pyruvate, 1 % nonessential amino acids, and 10 % fetal calf serum (FCS)). They were maintained at 37 °C in a humidified atmosphere gassed with 5 % CO_2 until cells grow out of the explants.

Alternatively, freshly dissociated PASMC were obtained using an enzymatic dissociation method already described [6]. Briefly, IPA pieces were placed successively in different dissociation solutions containing collagenase, papain, and dithioerythritol at 37 °C. Tissues were then gently agitated using a polished wide-bore Pasteur pipette to release the cells. Cells were then seeded on round glass coverslips, stored in serum-free culture medium enriched with 1 % insulin-transferrin-selenium (ITS), maintained at 37 °C in a humidified atmosphere gassed with 5 % CO_2, and used between 14 and 24 h after isolation.

Microspectrofluorimetric assay of cytosolic calcium

Before the experiments, PASMC were growth-arrested during 48 h by using serum-free culture medium supplemented with 1 % ITS. The Ca^{2+}-sensitive fluorescent probe indo-1 was used to record changes in $[Ca^{2+}]_i$. The cells plated on glass coverslips were incubated with 5 μM indo-1 penta-acetoxymethyl ester (indo-1/AM) in Krebs–HEPES solution (see composition below) at room temperature for 40 min, then washed and maintained at room temperature in the same saline solution before the fluorescence measurements.

For single cell measurements, the dual emission microspectrofluorimeter was constructed from a Nikon Diaphot inverted microscope fitted with epifluorescence (×40 oil immersion fluorescence objective; numerical aperture, 1.3). For excitation of indo-1, a collimated light beam from a 100-W mercury arc lamp (Nikon) was filtered at 355 nm and reflected from a dichroic mirror (380 nm). The emitted fluorescence signal was passed through a pinhole diaphragm slightly larger than the selected cell and directed onto another dichroic mirror (455 nm). Transmitted light was

filtered at 480 nm, reflected light was filtered at 405 nm, and the intensities were recorded by separate photometers (P100, Nikon). Under these experimental conditions, the fluorescence ratio (F_{405}/F_{480}) was calculated and recorded on-line as a voltage signal. $[Ca^{2+}]_i$ was estimated from the F_{405}/F_{480} using the formula derived by Grynkiewicz et al. [10] after Ca^{2+} calibration for indo-1 determined within cells as previously described [26].

In vitro migration assays

Modified Boyden chamber assay Modified Boyden chambers (BD Biosciences) containing 8 μm pore size membranes were positioned in 24-well tissue culture plates. After coating of the membranes with collagen, 25×10^3 cells were added to the top chamber in serum-free culture medium. The bottom chamber was filled with serum-free culture medium in the presence or absence of the agonists and the inhibitors. Next, after incubation for 24 h, to quantify migration through the porous membrane, cells were removed from the top side of the membrane mechanically using a cotton-tipped swab, and invading cells from the reverse side were fixed with methanol and stained with hematoxylin for 20 min. For each experiment, 15 representative pictures were taken for each insert, and then, cells were counted.

Wound-healing assay Cells (2×10^5) were seeded in a Petri dish and cultured in culture medium with 10 % FCS until confluence. Next, after incubation for 24 h in serum-free culture medium, a straight scratch was performed in the monolayer of cells using a pipette tip to obtain a wide acellular area. The medium was then replaced with the same medium containing or not the agonists and the inhibitors. After 24 h, cells were fixed with methanol and stained with hematoxylin for 20 min. Imaging of the two wound edges was performed (at four different positions along the scratch) and cells that migrated into the acellular area were counted.

In vitro proliferation assay

Briefly, cells were seeded at a density of 5×10^3 cells per well in a 96-well tissue culture plate and cultured in complete culture medium containing 10 % FCS. After 24 h, the medium was removed and replaced by a serum-free medium. After an additional period of 24 h at 37 °C, the medium was changed to complete culture medium containing 0.2 % serum in the presence or absence of the agonists. Following 24 h of incubation under these conditions, the media were removed and replaced with medium containing BrdU (10 μM), and cells were incubated for an additional 2 h at 37 °C. DNA synthesis was then assayed using Cell Proliferation ELISA, BrdU colorimetric method (Roche Applied Science), according to the manufacturer's instructions. Newly synthesized BrdU-DNA was determined using an EL808 ultra microplate reader (Bio-Tek Instruments) at a wavelength of 380 nm with a reference wavelength of 490 nm.

In vitro cell viability assay

Cells were seeded at a density of 5×10^3 cells per well in a standard 96-well tissue culture plate and cultured in complete culture medium containing 10 %. After 24 h, the medium was removed and replaced by a serum-free medium. After an additional period of 24 h at 37 °C, the medium was changed to complete culture medium containing 0.2 % serum in the presence or absence of the agonists. Following 24 h of incubation under these conditions, the water-soluble tetrazolium-1 (Wst-1, Roche Applied Science) was added to the media and cells were incubated for an additional 2 h at 37 °C. Cleavage of tetrazolium salt into formazan was determined, according to the manufacturer's instructions, using an EL808 ultra microplate reader (Bio-Tek Instruments) at a wavelength of 450 nm with a reference wavelength of 490 nm.

CML phenotype and TRPV immunostaining

After enzymatic dissociation, cells were seeded on eight-well chamber slides (Becton Dickinson) and grown in full medium containing 10 % FCS until confluence, prior to 24 h serum privation. Cells were washed twice in PBS and then fixed for 10 min in 4 % paraformaldehyde solution (Sigma). After fixation, cells were permeabilized with PBS containing 0.5 % Triton X-100 (Dutscher) for 5 min. Unspecific binding sites were blocked with PBS containing 4 % bovine serum albumin (BSA, Sigma) for 30 min. In order to validate smooth muscle cell phenotype, cells were labeled with a monoclonal anti-α smooth muscle actin (α-SMA) antibody (clone 1A4, 1:100, Sigma) and polyclonal calponin 1/2/3 (Santa Cruz) for 1 h in PBS–1 % BSA. In order to evaluate TRPV1 and TRPV4 expressions, cells were labeled with a polyclonal anti-TRPV1 antibody (Abcam) or a polyclonal anti-TRPV4 antibody (Abcam) for 1 h in PBS–1 % BSA. Cells were then washed with PBS and labeled with Alexa-Fluor 488 goat anti-mouse or Alexa-Fluor 568 goat anti-rabbit secondary antibody (1:200, Molecular Probes/Invitrogen) for 1 h in PBS–BSA 1 %. After the PBS wash, cell nuclei were stained with DAPI for 5 min (1:1,000, Sigma). Slides were then mounted with coverslips with an anti-fade Dako Fluorescent Mounting Medium (Dako) and then observed under a Nikon D-Eclipse C1 confocal scanning microscope using the Nikon Apo Plan×60/1.4NA oil immersion objective. Fluorescent images were acquired using the Nikon EZC1 software using the Helium-Blue Laser Diode (405 nm, for DAPI staining), the Helium-Neon Laser

Diode (543 nm, for Alexa-Fluor 568), and the Argon laser line (488 nm, for Alexa-Fluor 488), prior to analysis with the Nikon NIS-Elements software.

Cytoskeleton immunostaining

Briefly, cells were seeded on eight-well chamber slides (Becton Dickinson) and grown in full medium containing 10 % FCS until confluence, prior to 24 h 4α-PDD or capsaicin treatments in serum-free medium. At the end of the 24-h treatment, cells were washed twice in PBS and then fixed for 10 min in 4 % paraformaldehyde solution (Sigma). After fixation, cells were permeabilized with PBS containing 0.5 % Triton X-100 (Dutscher) for 5 min. Unspecific binding sites were blocked with PBS containing 4 % BSA (Sigma) for 30 min. In order to evaluate microtubule and intermediate filament networks, cells were labeled for 1 h in PBS–1 % BSA with a monoclonal anti-tubulin antibody (clone DM1A, 1:1,000, Sigma) or with a monoclonal anti-vimentin antibody (clone V9, 1:1,000, Sigma), respectively. Cells were then washed with PBS and labeled with Alexa-Fluor 488 goat anti-mouse secondary antibody (1:200, Molecular Probes/Invitrogen) for 1 h in PBS–BSA 1 %. After the PBS wash, cell nuclei were stained with DAPI for 5 min (1:1,000, Sigma). Slides were then mounted and observed as described above. Integrated density of fluorescent signal was determined using ImageJ software. Results were expressed as the percentage of integrated density of the mean of three different random images as compared to control untreated cells.

Recording solutions and application of drugs for microspectrofluorimetry studies

The standard Krebs–HEPES extracellular solution contained (in mM): 118.4 NaCl, 4.7 KCl, 2 $CaCl_2$, 1.2 $MgSO_4$, 4 $NaHCO_3$, 1.2 KH_2PO_4, 6 D-glucose, and 10 HEPES. The osmolality (measured with a cryoosmometer type 15 Löser) of the external salt solution was adjusted to 310 mOsm/kg with mannitol, and pH adjusted to 7.4 with NaOH.

The TRPV agonists, capsaicin and 4α-PDD, were applied to the recorded cell by pressure ejection from a glass pipette located close to the cell for the period indicated on the records. The TRPV antagonists, capsazepine and HC067047, were added to the extracellular solution 20 min before the application of agonists.

Reagents

General salts were from VWR. All other chemicals were purchased from Sigma, except DMEM–HEPES, FCS, and penicillin–streptomycin which were from Gibco (Invitrogen Corporation), and HC067047 which was from Tocris. 4α-PDD, capsaicin, capsazepine, and HC067047 were dissolved in dimethyl sulfoxide (DMSO) and diluted 1:2,000 into the bath to the final mentioned concentrations. At this dilution, the solvent (DMSO) alone had no effect on channel activity.

Data and statistical analysis

Results are expressed as mean ± SEM. Each experiment was repeated several times (n indicates the number of cells or rats). Mann–Whitney test or χ^2 test was used to determine statistical significance, and differences with $P < 0.05$ were considered significant.

Results

Expression of TRPV1 and TRPV4 mRNA and proteins

To verify the expression of TRPV1 and TRPV4, using specific primers (Table 1) and the RT-PCR technique, we first studied the expression of the mRNA in rat de-endothelialized IPA. PCR products, generated after 40 cycles, of the expected sizes (268 and 158 bp for TRPV1 and TRPV4, respectively) for the two subtypes were obtained consistently in three separate experiments and matched with those of positive controls generated from the brain (Fig. 1A).

As shown in Fig. 1B, western blot revealed expression of TRPV1 and TRPV4 proteins in rat de-endothelialized IPA. Specific anti-TRPV1 and anti-TRPV4 antibodies detected bands at≈100 kDa, consistently in six separate experiments. The size of these bands was in agreement with the predicted molecular mass of the two isoforms, 100 and 98 kDa for TRPV1 and TRPV4, respectively.

Functional activity of TRPV1 and TRPV4 channels

In order to investigate TRPV1 and TRPV4 at a functional level, we studied the effect of capsaicin and 4α-PDD, selective agonists of TRPV1 and TRPV4, respectively, on $[Ca^{2+}]_i$ in freshly dissociated (nonproliferating) rat PASMC (Fig. 1C). All the cells analyzed exhibited a stable resting $[Ca^{2+}]_i$. Application of capsaicin (10 μM) or 4α-PDD (5 μM) for 1 min elicited a fast increase in $[Ca^{2+}]_i$ (Fig. 1C(a)). As shown in Fig. 1C(b), in 60 % of tested cells (24 of 43 cells), capsaicin induced a $[Ca^{2+}]_i$ response in PASMC, the amplitude of which was 118±19 nM (n=24). In 71 % of tested cells (22 of 31 cells), activation of TRPV4 channels with 4α-PDD elicited a higher calcium response: 166±19 nM (n=22).

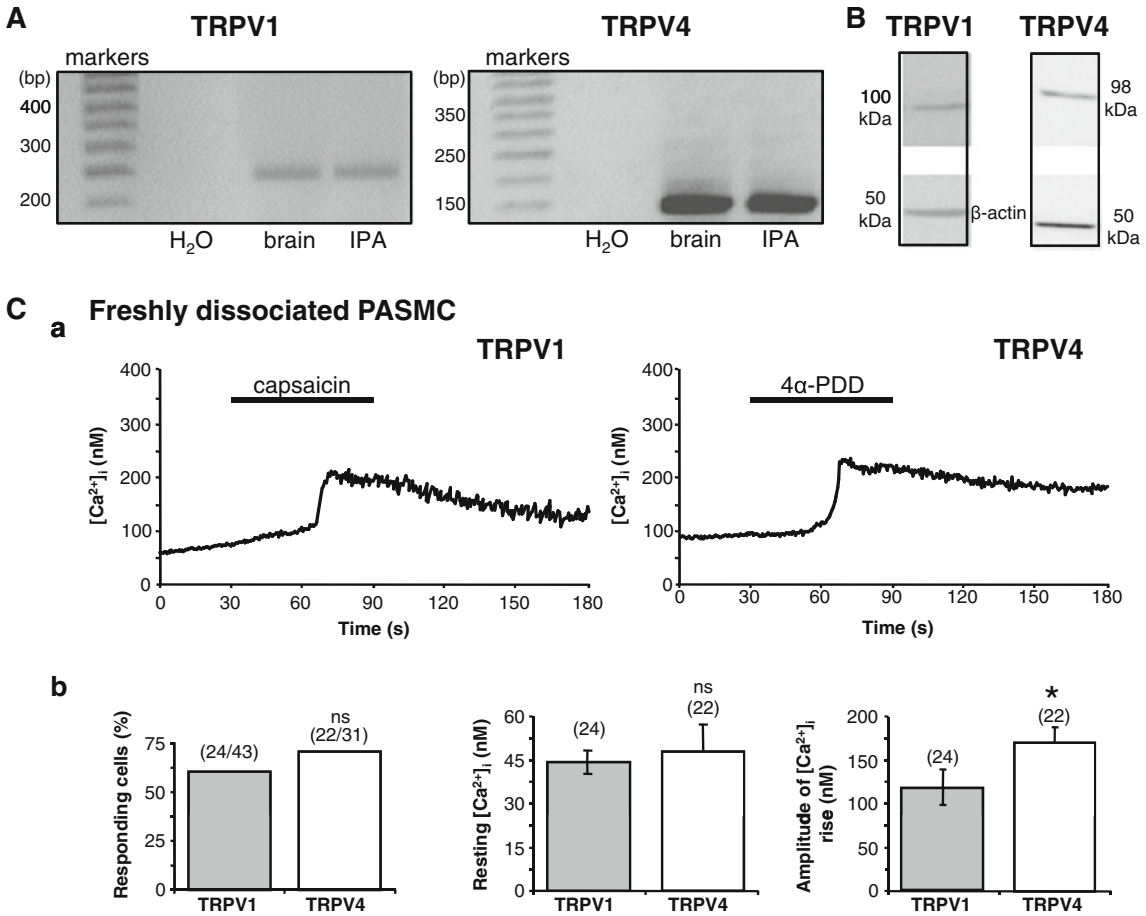

Fig. 1 Expression and functional activity of TRPV1 and TRPV4 channels in rat pulmonary arteries and freshly dissociated PASMC. **A** RT-PCR analysis of TRPV1 and TRPV4 channels in rat de-endothelialized intrapulmonary arteries (IPA) and brain. Brain mRNA was used as positive controls for TRPV1 and TRPV4. Negative controls were made by using water instead of cDNA. Expected lengths of PCR products are 268 and 158 bp for TRPV1 and TRPV4, respectively. **B** Western blot analysis of TRPV1 and TRPV4 channel expression in rat de-endothelialized intrapulmonary arteries. *Upper panels*: expression of proteins of interest. *Lower panels*: expression of β-actin. **C** $[Ca^{2+}]_i$ determination was carried out on single freshly dissociated PASMC using indo-1 as Ca^{2+} probe. Cells were bathed in recording medium containing 2 mM Ca^{2+}. *a* Typical recordings are shown when capsaicin (10 μM) or 4α-PDD (5 μM) was applied for the period indicated by the *horizontal bar*. *b* Percentages of responding cells, resting $[Ca^{2+}]_i$ values, and amplitude of the calcium rises in response to capsaicin (TRPV1) or 4α-PDD (TRPV4). Data are mean value ± SEM. The number of cells is indicated in *brackets*. Significant difference is indicated by *one asterisk* when $P<0.05$ and *ns* indicates a nonsignificant difference, $\chi 2$ or Mann–Whitney tests

Because PASMC can switch from a nonproliferative contractile phenotype to a proliferative "synthetic" phenotype and since this phenotypic transition and subsequent proliferation in pulmonary arteries contribute to PH [19], we assessed the effect of capsaicin and 4α-PDD on $[Ca^{2+}]_i$ in cultured (proliferating) rat PASMC (Fig. 2). All the cells analyzed exhibited a stable resting $[Ca^{2+}]_i$. Application of capsaicin (10 μM) or 4α-PDD (5 μM) for 1 min elicited a fast increase in $[Ca^{2+}]_i$ (Fig. 2A). As shown in Fig. 2B(a), in 19 % of tested cells (25 of 133 cells), capsaicin induced a $[Ca^{2+}]_i$ response in PASMC, the amplitude of which was 57±6 nM (n=25). In the presence of capsazepine (10 μM), reported to specifically block TRPV1, capsaicin-induced $[Ca^{2+}]_i$ rise was strongly reduced to an amplitude of 13±5 nM (n=4) in the only four responding cells out of 111 (Fig. 2B(a)), thus confirming that the capsaicin-induced calcium response was related to TRPV1 activation. In the same way, in 25 % of tested cells (17 of 68 cells), activation of TRPV4 channels with 4α-PDD elicited a calcium response: 136±17 nM (n=17) (Fig. 2B(b)). In the presence of HC067047 (5 μM), a specific inhibitor of TRPV4, the 4α-PDD-induced calcium response was reduced by 80 % (27±11 nM, n=4 of 64 cells) (Fig. 2B(b)), thus confirming that the 4α-PDD-induced calcium increase was related to TRPV4 activation. These present findings thus indicate that, whatever their phenotype (nonproliferative contractile or proliferative), PASMC express functional TRPV1 and TRPV4 channels.

Involvement of TRPV1 and TRPV4 channels in PASMC migration

Having shown that rat PASMC express functional TRPV1 and TRPV4 channels allowing $[Ca^{2+}]_i$ increase, we therefore

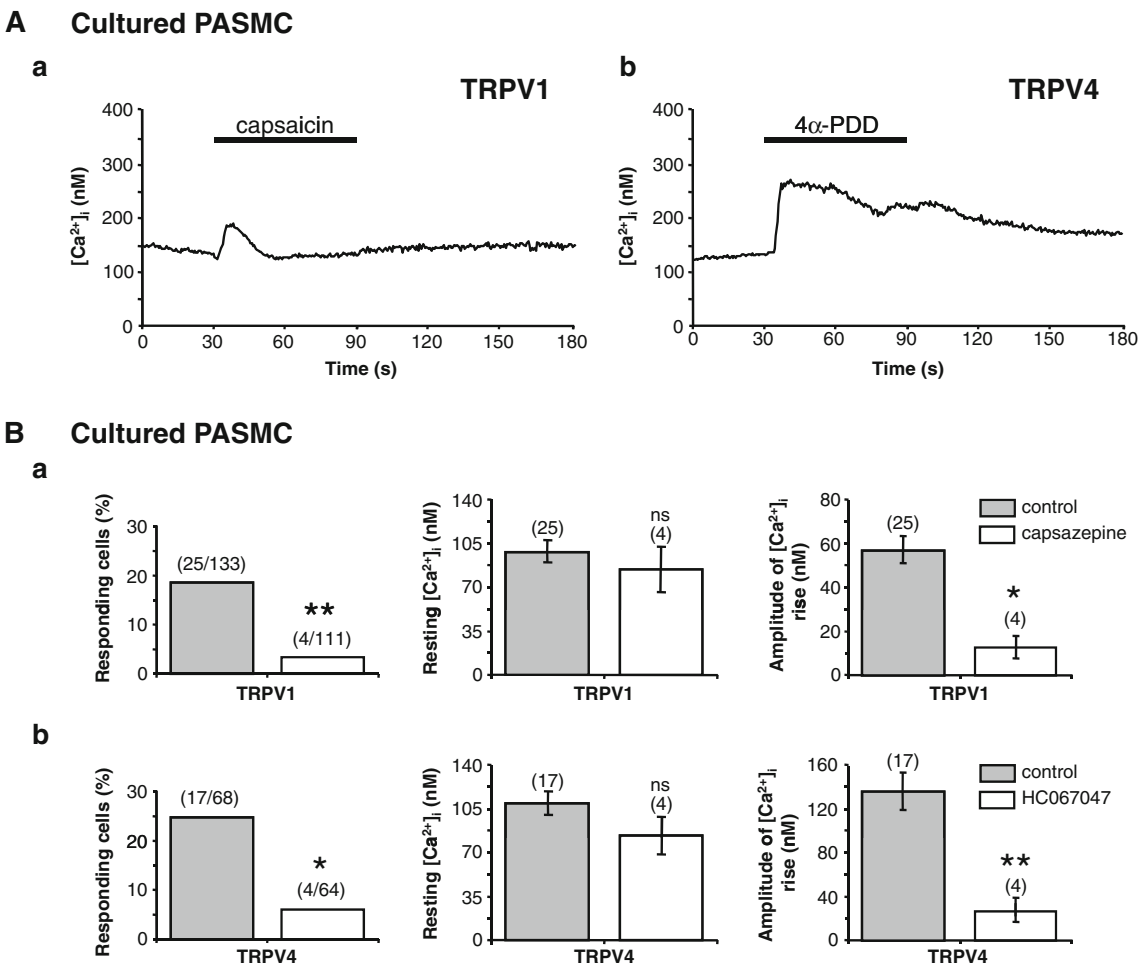

Fig. 2 Functional activity and pharmacological characterization of TRPV1 and TRPV4 channels in rat cultured PASMC. $[Ca^{2+}]_i$ determination was carried out on single cultured PASMC using indo-1 as Ca^{2+} probe. Cells were bathed in recording medium containing 2 mM Ca^{2+}. **A** Typical recordings are shown when *a* capsaicin (10 μM) or *b* 4α-PDD (5 μM) was applied for the period indicated by the *horizontal bar* in control conditions. **B** Percentages of responding cells, resting $[Ca^{2+}]_i$ values, and amplitude of the calcium rises in response to *a* capsaicin (TRPV1) or *b* 4α-PDD (TRPV4) in the absence (control conditions) or presence of the specific TRPV1 and TRPV4 inhibitors (capsazepine (10 μM) and HC067047 (5 μM), respectively). Data are mean value ± SEM. The number of cells is indicated in *brackets*. Significant difference is indicated by *one asterisk* when $P<0.05$, *two asterisks* when $P<0.001$, and *ns* indicates a nonsignificant difference, $\chi 2$ or Mann–Whitney tests

tested the ability of these channels to induce migration in PASMC. Figure 3A(a) illustrates the effects of capsaicin and 4α-PDD on PASMC migration as determined by the modified Boyden chamber assay. When cells were incubated with 10 μM capsaicin or 5 μM 4α-PDD for 24 h in serum-free DMEM, agonists significantly stimulated migration by 2.1- and 1.3-fold, respectively. As shown in Fig. 3A(b), similar results were obtained when we used the wound-healing assay. Treatment of PASMC with 10 μM capsaicin or 5 μM 4α-PDD for 24 h in serum-free DMEM increased cell migration by 176 and 70 %, respectively. These TRPV1- and TRPV4-induced migratory effects were inhibited by the addition of capsazepine (10 μM) or HC067047 (5 μM), respectively (Fig. 3A), confirming that these observed effects were related to TRPV1 and TRPV4 activation.

In another set of experiments, we verified that the observed change in cell migration was not due to increased cell growth. Using BrdU and Wst-1 colorimetric methods, we assessed the ability of capsaicin and 4α-PDD to increase cell proliferation and cellular growth/survival. As shown in Fig. 3B, whatever the method used, stimulation of cells with capsaicin (10 μM) or 4α-PDD (5 μM) for 24 h in low serum (0.2 % FCS) DMEM did not significantly increase cell proliferation or cellular viability, whereas the positive control (DMEM with 10 % FCS) did it.

Involvement of TRPV1 and TRPV4 channels in cytoskeleton reorganization

Since cell migration requires simultaneous changes in both cell morphology and adhesion, involving the formation of lamellipodia/pseudopodia, cell body contraction, and tail retraction [29], we investigated the effects of capsaicin and 4α-PDD on the cytoskeleton alteration. First, we confirmed

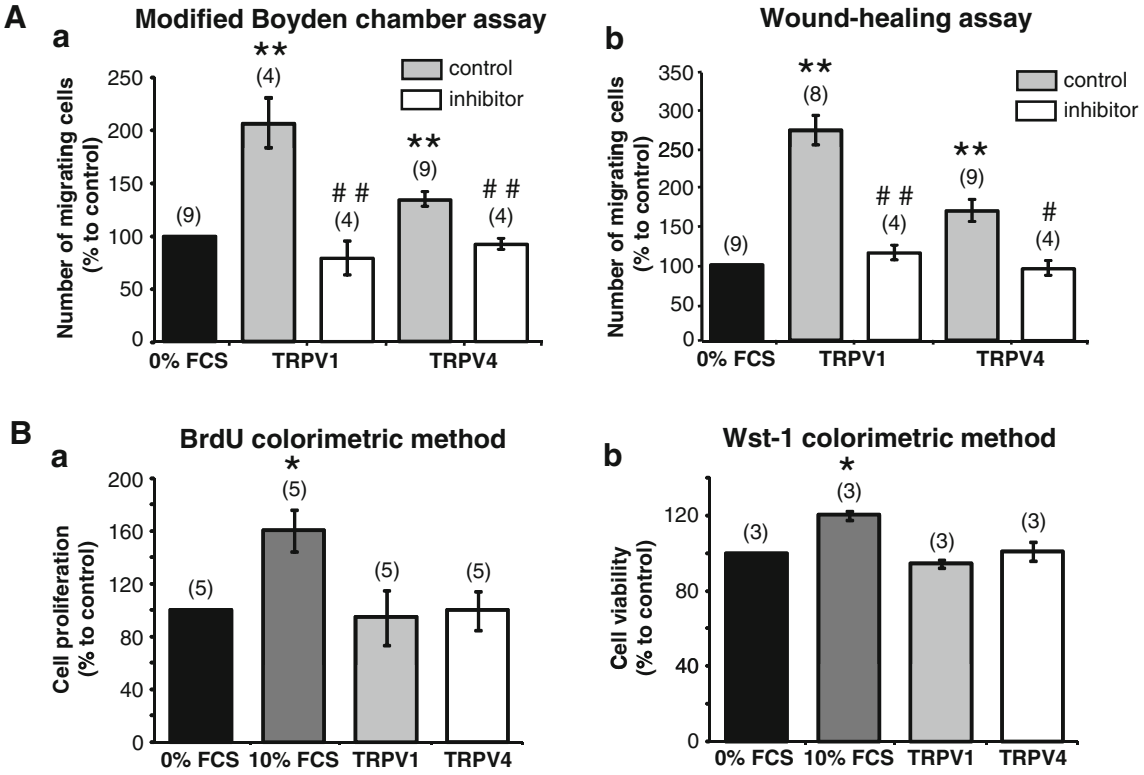

Fig. 3 Involvement of TRPV1 and TRPV4 channels in the migration of rat cultured PASMC. **A** Effects of capsaicin or 4α-PDD on rat PASMC migration evaluated by modified Boyden chamber (*a*) and wound-healing (*b*) assays. Cells were migrated in serum-free DMEM (control conditions, 0 % FCS), supplemented with 10 μM capsaicin (TRPV1/control), or 10 μM capsaicin with 10 μM capsazepine (TRPV1/inhibitor), or 5 μM 4α-PDD (TRPV4/control), or 5 μM 4α-PDD with 5 μM HC067047 (TRPV4/inhibitor) for 24 h. Results are expressed as a percentage of cells migrating in control conditions. Data are mean value ± SEM. The number of independent experiments is indicated in *brackets*. Significant difference between control conditions without capsaicin or 4α-PDD (0 % FCS) and control conditions with capsaicin or 4α-PDD (TRPV1/control and TRPV4/control, respectively) is indicated by *two asterisks* ($P<0.001$). Significant difference between capsaicin or 4α-PDD (TRPV1/control and TRPV4/control, respectively) and capsaicin plus capsazepine or 4α-PDD plus HC067047 (TRPV1/inhibitor and TRPV4/inhibitor, respectively) is indicated by *simple sharp* ($P<0.05$) or *double sharp* ($P<0.001$), Mann–Whitney test. **B** Effects of capsaicin or 4α-PDD on rat PASMC proliferation (*a*) and viability (*b*) evaluated by BrdU and Wst-1 colorimetric methods, respectively. Cell proliferation was assessed by quantitative determination of DNA synthesis using the Cell Proliferation ELISA BrdU colorimetric method. Cell viability was assessed by the colorimetric water-soluble tetrazolium-1 assay, based on living cells' cleavage of tetrazolium salt into formazan. Cells were incubated for 24 h in DMEM containing 0.2 % FCS (control conditions, 0 % FCS) supplemented with 10 μM capsaicin (TRPV1) or 5 μM 4α-PDD (TRPV4), or DMEM containing 10 % FCS before BrdU or Wst-1 incubation. Data are mean value ± SEM. The number of independent experiments is indicated in *brackets*. Significant difference from control conditions is indicated by *one asterisk* ($P<0.05$), Mann–Whitney test

that cultured PASMC were a homogenous cell population. As shown in immunostaining experiments, cells expressed both α-SMA (Fig. 4F–H) and calponin (Fig. 4J), well-known smooth muscle cell markers. In order to determine if cultured PASMC expressed TRPV1 and TRPV4 channels, we performed immunostaining using TRPV1 and TRPV4 antibodies (Fig. 4K, L). Co-immunostaining with α-SMA (Fig. 4G, H) revealed that all PASMC were TRPV1 and TRPV4 positive (Fig. 4O, P).

Second, TRPV1 and TRPV4-induced cytoskeletal changes were investigated using immunostaining experiments. In control cells (Fig. 5A), staining of actin cytoskeleton with an anti-α smooth muscle actin antibody was diffused throughout the cell and cells displayed actin stress fibers generally parallel to the longitudinal axis. The density of the actin filament network increased in the cell periphery. Stimulation of cells with 10 μM capsaicin (Fig. 5B) or 5 μM 4α-PDD (Fig. 5C) for 24 h significantly increased the intensity of the staining by 2.0- and 3.9-fold, respectively, as compared to control staining (Fig. 5D). These results suggested that TRPV1 and TRPV4 stimulations were associated with changes in the actin architecture. Staining for tubulin showed that the microtubule network was specifically reorganized and increased in the presence of TRPV4 agonist (Fig. 5H). Indeed, in untreated cells (Fig. 5E), the staining was organized in a fine network from punctuate staining. In the presence of 5 μM 4α-PDD (Fig. 5G), the staining of the tubulin network was more intense, whereas no significant changes were observed upon capsaicin treatment (Fig. 5F). Finally, staining for vimentin revealed that intermediate filament network was organized in a fine network from perinuclear areas (Fig. 5I). Incubation with

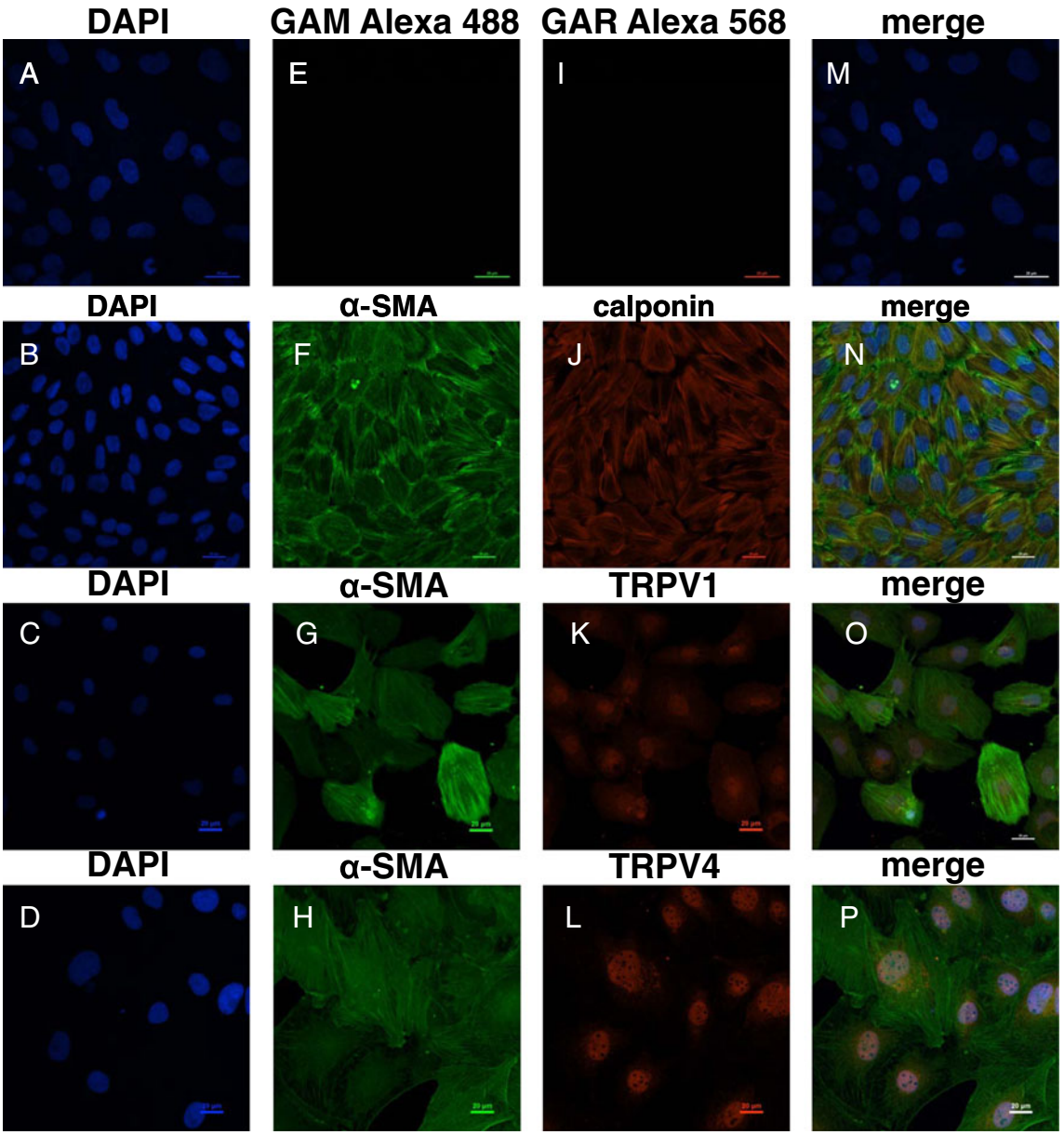

Fig. 4 Expression of smooth muscle cell markers, TRPV1 and TRPV4 channels in rat cultured PASMC. Representative confocal immunofluorescence fields of control cells. **a–D** Cell nuclei were stained with DAPI. **E** Cells were stained with an Alexa-Fluor 488-conjugated antibody. **F–H** Cells were stained with a primary antibody for α smooth muscle actin (α-SMA) and an Alexa-Fluor 488-conjugated secondary antibody. **I** Cells were stained with an Alexa-Fluor 568-conjugated antibody. **J** Cells were stained with a primary antibody for calponin and an Alexa-Fluor 568-conjugated secondary antibody. **K** Cells were stained with a primary antibody for TRPV1 and an Alexa-Fluor 568-conjugated secondary antibody. **L** Cells were stained with a primary antibody for TRPV4 and an Alexa-Fluor 568-conjugated secondary antibody. **M–P** Merging images. All images were taken with the same illumination time. Experiments were performed on four independent cell preparations from four rats. *Scale bar*=20 μm

10 μM capsaicin for 24 h increased the intensity of the staining which was denser in the nuclear periphery (Fig. 5J, L), whereas 4α-PDD treatment was ineffective (Fig. 5K, L). In conclusion, the present results indicate that TRPV1 and TRPV4 stimulations of PASMC are associated with specific changes in the cytoskeleton architecture, and the intracellular distribution and/or expression of cytoskeletal proteins is visibly altered.

Discussion

In the present work, using reverse transcriptase–polymerase chain reaction and western blot analysis, we confirm the expression of TRPV1 and TRPV4 channels in rat PASMC. We also show that these isoforms can be activated by capsaicin and 4α-PDD, selective TRPV1 and TRPV4 agonists, respectively, which leads to intracellular Ca^{2+} increase,

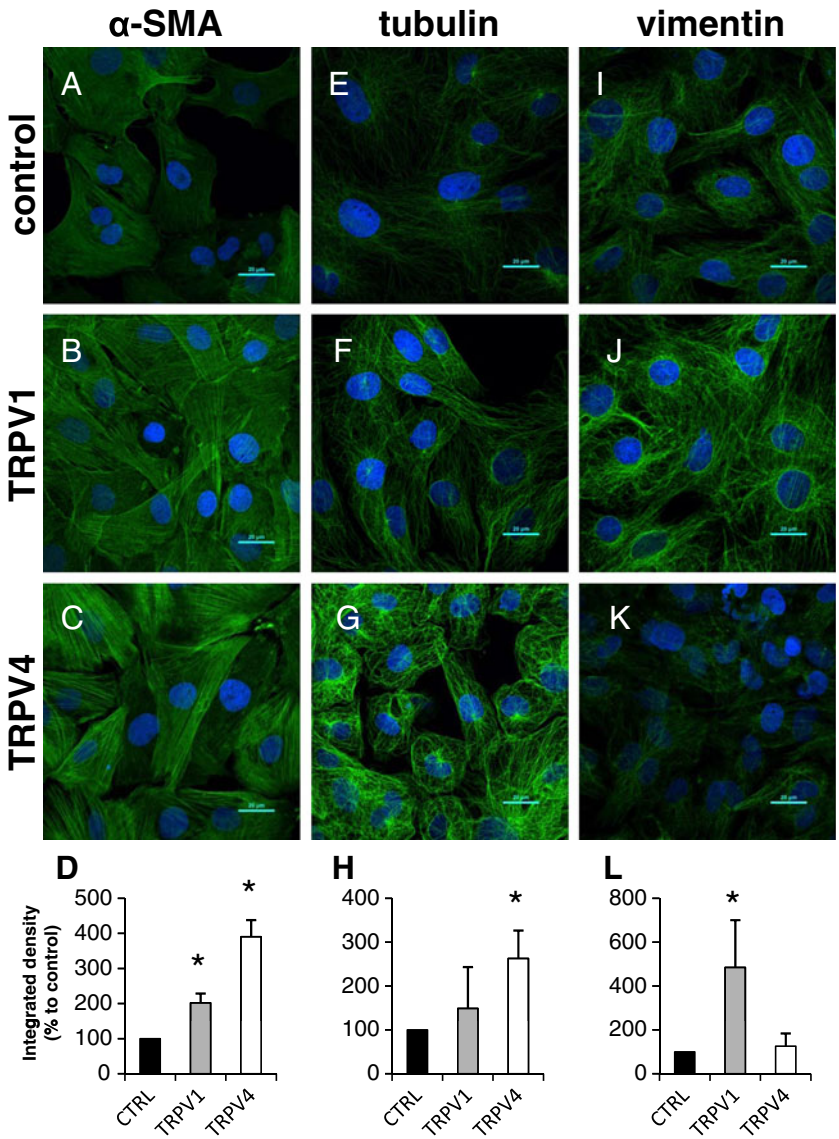

Fig. 5 Involvement of TRPV1 and TRPV4 channels in the cytoskeleton reorganization of rat cultured PASMC. Representative confocal immunofluorescence fields of control cells (*upper panels*, control) and cells treated with 10 μM capsaicin (*middle panels*, TRPV1) or 5 μM 4α-PDD (*lower panels*, TRPV4) for 24 h on cytoskeleton reorganization. **A–C** Cells were stained with a primary antibody for α smooth muscle actin (α-SMA) and an Alexa-Fluor 488-conjugated secondary antibody. **E–G** Microtubule network stained with a primary antibody for tubulin and an Alexa-Fluor 488-conjugated secondary antibody. **i–K** Intermediate filament network stained with a primary antibody for vimentin and an Alexa-Fluor 488-conjugated secondary antibody. Quantification of fluorescence is expressed as a percentage of integrate density of untreated cells (control cells, CTRL) for α-SMA (*D*), tubulin (*H*), and vimentin (*L*). Cell nuclei were stained with DAPI. All images were taken with the same illumination time. Experiments were performed on four independent cell preparations from four rats. *Scale bar*=20 μm

indicating that these channels are functional Ca^{2+} channels. In addition, to the best of our knowledge, we also provide, for the first time, a direct proof, at a single cell level, that stimulation of TRPV1 and TRPV4 channels enhances the migration of PASMC, a crucial step in the progression of PH [27].

Despite their implication in numerous physiological functions in smooth muscle cells [12], whatever the type of cells, the involvement of TRPV channels in migration is much more elusive. It has been reported that TRPV1 stimulates migration of human hepatoblastoma (HepG2) cells [33], human corneal epithelial cells [36], and mouse dendritic cells [1]. The involvement of TRPV2 in human prostate (LNCaP) cell migration [23] and TRPV4 in endothelial cell migration [7] was also described. Finally, on the contrary, TRPV1 and TRPV4 inhibit migration in urothelial cancer and neuroendocrine cells, respectively [3, 38]. Our data thus indicate that activation of these channels favors migration in PASMC.

Interestingly, in human and rat PASMC, chronic hypoxia up-regulates expression levels of the TRPV1 and TRPV4 gene and protein [32, 37]. In the same way, we recently demonstrated that the activity of stretch-activated channels in rat PASMC was increased under chronic hypoxia [6], an effect that can be ascribed to TRPV1 and TRPV4 activity since they have been demonstrated to exhibit mechanosensitivity [16, 20, 22, 30]. Moreover, we also previously showed that serotonin, whose plasma concentration is increased in PH [13] and which stimulates bovine PASMC migration [4], activates a TRPV4-like current in rat PASMC [5]. Based on these findings, we can thus assume that the variation of expression and/or activity of these channels may be an early step leading to cell migration observed in PH.

Most likely, the increase in the $[Ca^{2+}]_i$ following the Ca^{2+} influx via TRPV channels plays a key role in this process. Indeed, cell migration is a multifactorial and multistep process and many of its components are regulated by the

$[Ca^{2+}]_i$ [14, 21]. Moreover, it has been proposed that stretch-activated channels could play a crucial role in mediating localized Ca^{2+} rise needed for migration [18, 34]. Nonetheless, herein, the fact that the migratory response is more important for TRPV1 than for TRPV4, whereas the reverse is true concerning the amplitude of the calcium response, suggests that Ca^{2+} is not the only actor in the signaling cascade. Interestingly, Goswami's group recently provided evidence that TRPV1 and TRPV4 directly interact with microtubules [8, 9]. Activation of these channels results in a selective depolymerization of microtubules, although the mechanism by which this occurs still remains unclear. Moreover, TRPV4 also interacts with actin whereas TRPV1 does not, which could account for the differences in agonist-induced cytoskeleton reorganization observed in our study.

Finally, our results regarding stimulation of migration by TRPV1 and TRPV4 activation cannot be attributed to a proliferative effect in rat PASMC. Although a recent study suggests that TRPV1 may be a critical mediator in chronic hypoxia-induced proliferation of human PASMC [32], this result was derived from experiments in which TRPV1 was solely inhibited. However, under such conditions, as discussed by the authors, TRPV1 may have induced a proliferative effect via formation of the heterotetrameric channel.

In conclusion, this study demonstrates the expression of TRPV1 and TRPV4 and their role as Ca^{2+} channel involved in the migration of rat PASMC. Consequently, these channels may represent a relevant target for the treatment of vascular diseases such as pulmonary hypertension. In particular, these channels may contribute to link stretch-induced effect and vessel remodeling.

Acknowledgments The authors thank Dr. V. Michel and S. Marais for their helpful technical advice. This work was supported by the Fondation de France [2008002719].

References

1. Basu S, Srivastava P (2005) Immunological role of neuronal receptor vanilloid receptor 1 expressed on dendritic cells. Proc Natl Acad Sci U S A 102:5120–5
2. Billaud M, Marthan R, Savineau JP, Guibert C (2009) Vascular smooth muscle modulates endothelial control of vasoreactivity via reactive oxygen species production through myoendothelial communications. PLoS One 4:e6432
3. Caprodossi S, Amantini C, Nabissi M, Morelli MB, Farfariello V, Santoni M, Gismondi A, Santoni G (2011) Capsaicin promotes a more aggressive gene expression phenotype and invasiveness in null-TRPV1 urothelial cancer cells. Carcinogenesis 32:686–94
4. Day RM, Agyeman AS, Segel MJ, Chevere RD, Angelosanto JM, Suzuki YJ, Fanburg BL (2006) Serotonin induces pulmonary artery smooth muscle cell migration. Biochem Pharmacol 71: 386–97
5. Ducret T, Guibert C, Marthan R, Savineau JP (2008) Serotonin-induced activation of TRPV4-like current in rat intrapulmonary arterial smooth muscle cells. Cell Calcium 43:315–23
6. Ducret T, El Arrouchi J, Courtois A, Quignard JF, Marthan R, Savineau JP (2010) Stretch-activated channels in pulmonary arterial smooth muscle cells from normoxic and chronically hypoxic rats. Cell Calcium 48:251–9
7. Fiorio Pla A, Ong HL, Cheng KT, Brossa A, Bussolati B, Lockwich T, Paria B, Munaron L, Ambudkar IS (2011) TRPV4 mediates tumor-derived endothelial cell migration via arachidonic acid-activated actin remodeling. Oncogene 31(2):200–12
8. Goswami C, Dreger M, Otto H, Schwappach B, Hucho F (2006) Rapid disassembly of dynamic microtubules upon activation of the capsaicin receptor TRPV1. J Neurochem 96:254–66
9. Goswami C, Kuhn J, Heppenstall PA, Hucho T (2010) Importance of non-selective cation channel TRPV4 interaction with cytoskeleton and their reciprocal regulations in cultured cells. PLoS One 5: e11654
10. Grynkiewicz G, Poenie M, Tsien RY (1985) A new generation of Ca2+ indicators with greatly improved fluorescence properties. J Biol Chem 260:3440–50
11. Guibert C, Ducret T, Savineau JP (2008) Voltage-independent calcium influx in smooth muscle. Prog Biophys Mol Biol 98:10–23
12. Guibert C, Ducret T, Savineau JP (2011) Expression and physiological roles of TRP channels in smooth muscle cells. Adv Exp Med Biol 704:687–706
13. Herve P, Launay JM, Scrobohaci ML, Brenot F, Simonneau G, Petitpretz P, Poubeau P, Cerrina J, Duroux P, Drouet L (1995) Increased plasma serotonin in primary pulmonary hypertension. Am J Med 99:249–54
14. House SJ, Potier M, Bisaillon J, Singer HA, Trebak M (2008) The non-excitable smooth muscle: calcium signaling and phenotypic switching during vascular disease. Pflugers Arch 456: 769–85
15. Humbert M, Morrell NW, Archer SL, Stenmark KR, MacLean MR, Lang IM, Christman BW, Weir EK, Eickelberg O, Voelkel NF, Rabinovitch M (2004) Cellular and molecular pathobiology of pulmonary arterial hypertension. J Am Coll Cardiol 43:13S–24S
16. Inoue R, Jian Z, Kawarabayashi Y (2009) Mechanosensitive TRP channels in cardiovascular pathophysiology. Pharmacol Ther 123:371–85
17. Jeffery TK, Wanstall JC (2001) Pulmonary vascular remodelling in hypoxic rats: effects of amlodipine, alone and with perindopril. Eur J Pharmacol 416:123–31
18. Lee J, Ishihara A, Oxford G, Johnson B, Jacobson K (1999) Regulation of cell movement is mediated by stretch-activated calcium channels. Nature 400:382–6
19. Liang W, Ray JB, He JZ, Backx PH, Ward ME (2009) Regulation of proliferation and membrane potential by chloride currents in rat pulmonary artery smooth muscle cells. Hypertension 54:286–93
20. Loukin S, Zhou X, Su Z, Saimi Y, Kung C (2010) Wild-type and brachyolmia-causing mutant TRPV4 channels respond directly to stretch force. J Biol Chem 285:27176–81
21. Mandegar M, Fung YC, Huang W, Remillard CV, Rubin LJ, Yuan JX (2004) Cellular and molecular mechanisms of pulmonary vascular remodeling: role in the development of pulmonary hypertension. Microvasc Res 68:75–103
22. Mochizuki T, Sokabe T, Araki I, Fujishita K, Shibasaki K, Uchida K, Naruse K, Koizumi S, Takeda M, Tominaga M (2009) The TRPV4 cation channel mediates stretch-evoked Ca2+ influx and ATP release in primary urothelial cell cultures. J Biol Chem 284: 21257–64
23. Monet M, Lehen'kyi V, Gackiere F, Firlej V, Vandenberghe M, Roudbaraki M, Gkika D, Pourtier A, Bidaux G, Slomianny C, Delcourt P, Rassendren F, Bergerat JP, Ceraline J, Cabon F, Humez S, Prevarskaya N (2010) Role of cationic channel TRPV2 in promoting prostate cancer migration and progression to androgen resistance. Cancer Res 70:1225–35

24. Muraki K, Iwata Y, Katanosaka Y, Ito T, Ohya S, Shigekawa M, Imaizumi Y (2003) TRPV2 is a component of osmotically sensitive cation channels in murine aortic myocytes. Circ Res 93:829–38
25. Nilius B, Vriens J, Prenen J, Droogmans G, Voets T (2004) TRPV4 calcium entry channel: a paradigm for gating diversity. Am J Physiol Cell Physiol 286:C195–205
26. Pauvert O, Bonnet S, Rousseau E, Marthan R, Savineau JP (2004) Sildenafil alters calcium signaling and vascular tone in pulmonary arteries from chronically hypoxic rats. Am J Physiol Lung Cell Mol Physiol 287:L577–83
27. Pietra GG, Capron F, Stewart S, Leone O, Humbert M, Robbins IM, Reid LM, Tuder RM (2004) Pathologic assessment of vasculopathies in pulmonary hypertension. J Am Coll Cardiol 43:25S–32S
28. Rabinovitch M, Gamble W, Nadas AS, Miettinen OS, Reid L (1979) Rat pulmonary circulation after chronic hypoxia: hemodynamic and structural features. Am J Physiol 236:H818–27
29. Ridley AJ, Schwartz MA, Burridge K, Firtel RA, Ginsberg MH, Borisy G, Parsons JT, Horwitz AR (2003) Cell migration: integrating signals from front to back. Science 302:1704–9
30. Spencer NJ, Kerrin A, Singer CA, Hennig GW, Gerthoffer WT, McDonnell O (2008) Identification of capsaicin-sensitive rectal mechanoreceptors activated by rectal distension in mice. Neuroscience 153:518–34
31. Wang J, Shimoda LA, Sylvester JT (2004) Capacitative calcium entry and TRPC channel proteins are expressed in rat distal pulmonary arterial smooth muscle. Am J Physiol Lung Cell Mol Physiol 286:L848–58
32. Wang YX, Wang J, Wang C, Liu J, Shi LP, Xu M, Wang C (2008) Functional expression of transient receptor potential vanilloid-related channels in chronically hypoxic human pulmonary arterial smooth muscle cells. J Membr Biol 223:151–9
33. Waning J, Vriens J, Owsianik G, Stuwe L, Mally S, Fabian A, Frippiat C, Nilius B, Schwab A (2007) A novel function of capsaicin-sensitive TRPV1 channels: involvement in cell migration. Cell Calcium 42:17–25
34. Wei C, Wang X, Chen M, Ouyang K, Song LS, Cheng H (2009) Calcium flickers steer cell migration. Nature 457:901–5
35. Yang XR, Lin MJ, McIntosh LS, Sham JS (2006) Functional expression of transient receptor potential melastatin- and vanilloid-related channels in pulmonary arterial and aortic smooth muscle. Am J Physiol Lung Cell Mol Physiol 290:L1267–76
36. Yang H, Wang Z, Capo-Aponte JE, Zhang F, Pan Z, Reinach PS (2010) Epidermal growth factor receptor transactivation by the cannabinoid receptor (CB1) and transient receptor potential vanilloid 1 (TRPV1) induces differential responses in corneal epithelial cells. Exp Eye Res 91:462–71
37. Yang XR, Lin AH, Hughes JM, Flavahan NA, Cao YN, Liedtke W, Sham JS (2012) Upregulation of osmo-mechanosensitive TRPV4 channel facilitates chronic hypoxia-induced myogenic tone and pulmonary hypertension. Am J Physiol Lung Cell Mol Physiol 302:L555–68
38. Zaninetti R, Fornarelli A, Ciarletta M, Lim D, Caldarelli A, Pirali T, Cariboni A, Owsianik G, Nilius B, Canonico PL, Distasi C, Genazzani AA (2011) Activation of TRPV4 channels reduces migration of immortalized neuroendocrine cells. J Neurochem 116:606–15